Investigation of Cu-doped $Li_2B_4O_7$ single crystals by electron paramagnetic resonance and time-resolved optical spectroscopy

2008 J. Phys.: Condens. Matter 20 025216

(http://iopscience.iop.org/0953-8984/20/2/025216)

J. Phys.: Condens. Matter **20** (2008) 025216 (9pp) doi:10.1088/0953-8984/20/02/025216

Investigation of Cu-doped $Li_2B_4O_7$ single crystals by electron paramagnetic resonance and time-resolved optical spectroscopy

G Corradi[1], V Nagirnyi[2,5], A Kotlov[2], A Watterich[1], M Kirm[2], K Polgár[1], A Hofstaetter[3] and M Meyer[4]

[1] Research Institute for Solid State Physics and Optics, Hungarian Academy of Sciences, Budapest, POB 49, H-1525, Hungary
[2] Institute of Physics, University of Tartu, 142 Riia Street, 51014 Tartu, Estonia
[3] I. Physikalisches Institut, University of Giessen, D-35392 Giessen, Germany
[4] Physics Department, Osnabrück University, D-49069 Osnabrück, Germany

E-mail: vetal@fi.tartu.ee

Received 26 June 2007, in final form 25 October 2007
Published 6 December 2007
Online at stacks.iop.org/JPhysCM/20/025216

Abstract
A low-temperature study of the thermoluminescent dosimeter material, lithium tetraborate ($Li_2B_4O_7$) doped by Cu, has been carried out by the methods of electron paramagnetic resonance (EPR) and time-resolved polarization spectroscopy using 4–20 eV synchrotron radiation and 1 μs Xe flash lamp pulses in the region 3–6 eV. The observed EPR spectra of an unpaired hole with strong d-character and characteristic hyperfine splittings can be ascribed to Cu^{2+} substituted at a Li lattice site and displaced due to relaxation. The results on the Cu^+-related luminescence strongly support the conclusion about a low-symmetry position of copper impurity ions in the lithium tetraborate lattice. The temperature dependence of the decay kinetics of the Cu^+-related 3.35 eV emission indicates a triplet nature for the relaxed excited state of the Cu^+ centres. An off-centre position of the Cu^+ ion in the relaxed excited state is suggested.

1. Introduction

Lithium tetraborate ($Li_2B_4O_7$) is an acousto- and optoelectronic material widely used for nonlinear optical applications in the ultraviolet (UV) region due to its transparency extending as far as 160 nm, which is remarkable even among other borates. Its crystal structure is characterized by the space group $I4_1cd$ belonging to the point group C_{4v}, and can be described as a =B–O–B≡ covalent network consisting of a frame of alternating oxygen-bonded BO_4 and BO_3 oxyanions and stabilized by Li^+ ions accommodated within this network [1]. The basic structural unit of the network is a cradle-like B_4O_7 group (see figure 1). The lowest-energy electronic excitations, leading to transitions from oxygen to boron oxyanionic states, efficiently form self-trapped excitons (STEs) in this material, which decay radiatively resulting in a characteristic STE emission at 3.65 eV (see, e.g., [2, 3] and references therein). Intrinsic defects introduced by neutron irradiation have been characterized earlier by EPR [4, 5].

If activated by small amounts of Cu, $Li_2B_4O_7$ has been known as a tissue-equivalent thermoluminescent dosimeter whose properties can be further improved by using appropriate co-dopants, leading to an outstanding sensitivity exceeding that of the well-known LiF:Mg,Ti phosphor [6]. However, no studies characterizing the incorporation sites of any dopants in $Li_2B_4O_7$ have so far been reported. Neither have the luminescence properties of $Li_2B_4O_7$:Cu been sufficiently investigated. The studies have mostly been carried out on polycrystalline or glassy samples and confined to room temperature and a narrow range of excitation energies in the UV ($E_{exc} < 6$ eV), insufficient to reveal the variety of

[5] Author to whom any correspondence should be addressed.

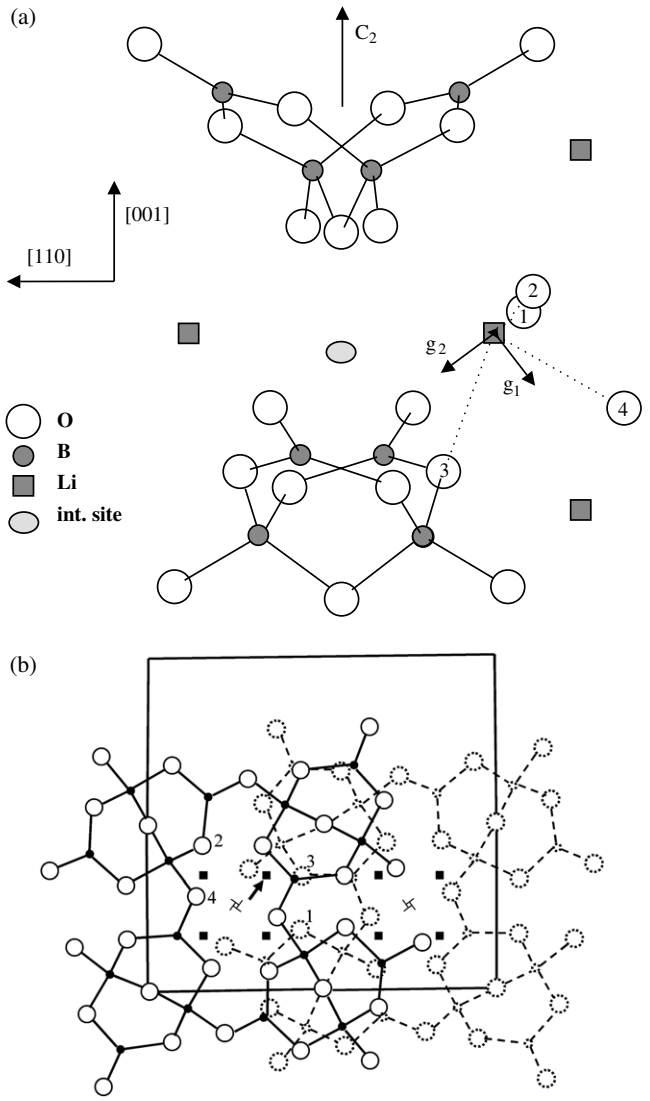

Figure 1. Structure of the $Li_2B_4O_7$ lattice [1] shown as projections of part of the tetragonal elementary cell along a [110]-type axis (a) and along the [001] or *c* axis (b), also showing the ≡B–O–B≡ covalent network. Some positions of the twofold C_2 and the vertical fourfold screw axes, as well as a possible interstitial Cu^+ site on the C_2 axis, are also indicated. The nearest oxygen neighbours of a chosen Li site (indicated by an arrow in part (b)) are numbered 1–4. The principal directions of the Cu^{2+}**g** tensor given in table 1 are indicated in part (a). Note that the main principal axis is nearly perpendicular to the plane of the projection.

impurity states which might be involved, taking into account the large energy gap of the material. Photo- or electron-excited luminescence has recently been reported for single crystals, showing a 370 nm (3.35 eV) characteristic emission band attributed to Cu^+ ions [7, 8].

In the present paper we report on EPR studies on Cu^{2+} ions and a parallel low-temperature optical study of $Li_2B_4O_7$:Cu single crystals based on time-resolved polarization spectroscopy using synchrotron radiation in the 4–20 eV region and microsecond Xe flash lamp pulses in the 3–6 eV region. The investigation is aimed at obtaining information on substitution sites of dopants like Cu^{2+} and Cu^+ ions introduced in the $Li_2B_4O_7$ matrix and at understanding the processes of relaxation of electronic excitations and energy transport to the recombination centres relevant for dosimetric applications of the material studied.

2. Experimental details

$Li_2B_4O_7$ single crystals containing, according to an atomic absorption analysis, $\sim 4 \times 10^{-3}$ mol% Cu have been prepared using the Czochralski method at the Research Institute for Solid State Physics and Optics, Budapest, Hungary. The crystals contained both Cu^{2+} and Cu^+ ions in an undefined ratio.

EPR spectra were recorded using ESP-300 Bruker spectrometers in the X and Q bands at the Universities of Osnabrück and Giessen. The spectra taken in the Q band yielded no additional information and are not reported here.

The synchrotron radiation study of $Li_2B_4O_7$:Cu crystals in the energy region 4–20 eV was performed at the SUPERLUMI station of HASYLAB, Hamburg, Germany, taking advantage of the natural polarization of the synchrotron radiation in the horizontal plane. Excitation and absorption spectra were measured from oriented samples in nearly normal (incidence angle 17°) and normal incidence geometry, respectively. The absorption spectra in the region 4–8 eV were measured using an AXUV-100 photodiode. The emission was analysed with a SpectraPro308i (Acton) spectrograph and a Hamamatsu PMT R6358P. All necessary corrections have been introduced into the emission and excitation spectra. For the photon energies used, no effects indicating charge transfer have been observed.

Time-resolved polarization spectroscopic measurements in the energy region 3–6 eV were performed at the Institute of Physics, University of Tartu, Estonia. The methods for measuring emission and excitation spectra, as well as the emission decay kinetics, have been described elsewhere [9]. An Ahrens prism was used for the analysis of emission polarization properties. Two intensities were measured, with the analyser parallel ($I_\parallel$) and perpendicular ($I_\perp$) to the **c** axis of the crystal. The degree of polarization was calculated as $P = 100\% \times (I_\parallel - I_\perp)/(I_\parallel + I_\perp)$. The polarization was considered positive in the case of $I_\parallel > I_\perp$, and negative in the case of $I_\parallel < I_\perp$.

3. Results and discussion

3.1. EPR results

The EPR spectra could be observed in the temperature region 6–180 K, showing a normal Curie-like temperature dependence without structural changes but saturating towards lower temperatures (figure 2). The power dependence also passes through a maximum, as expected for inhomogeneously broadened lines (figure 2 insets). A convenient temperature chosen for a detailed study was near 30 K.

All major features of the spectra could be explained by the $S = 1/2$ spin-Hamiltonians of Cu^{2+} ions

$$\mathcal{H}_i = \mu_B \boldsymbol{S}\mathbf{g}\boldsymbol{B} + \boldsymbol{S}\mathbf{A}_i\boldsymbol{I}_i,$$

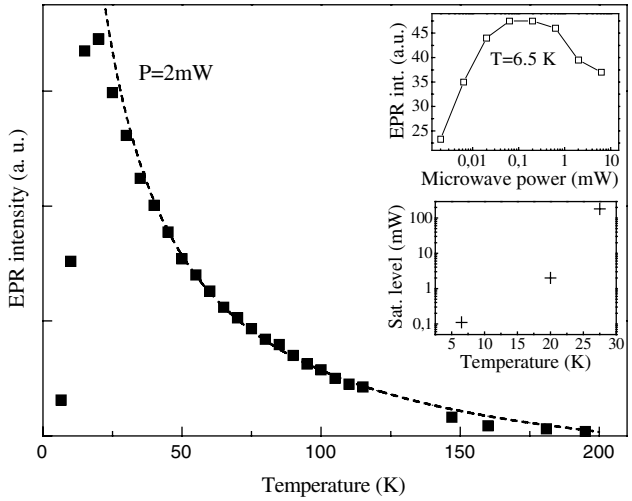

Figure 2. Temperature dependence of the Cu^{2+} EPR signal intensity at the microwave power $P = 2$ mW, showing an approximate $1/T$ dependence and saturating at low temperatures (main plot), saturation behaviour of the EPR signal for $T = 6.5$ K (upper inset), and the temperature dependence of the saturation power level corresponding to maximal EPR intensity (lower inset).

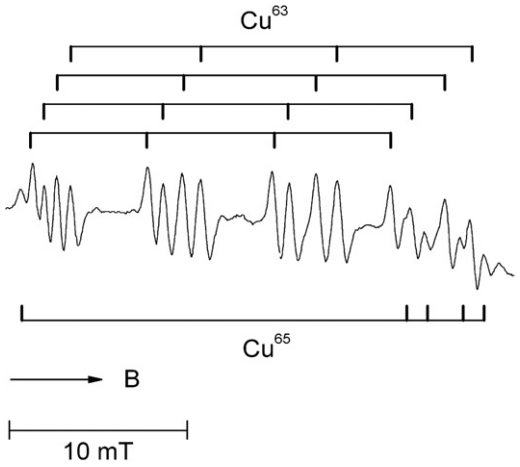

Figure 3. Resolved hyperfine structure of the four high-field EPR lines (X band) due to the isotopes Cu^{63} and Cu^{65}. The magnetic field, parallel within a few degrees to the xz plane, makes an angle of ~58° with the z axis.

Table 1. Principal values and eigenvector coordinates of the spin-Hamiltonian tensors. The $\mathbf{A}^{63}$ values are given in units of 10^{-4} cm^{-1}. The estimated errors of the directions are ±2° and ±4° for the g and HF eigenvectors, respectively.

g tensor		
2.515 ± 0.013	2.220 ± 0.010	2.0265 ± 0.0010
0.423	0.551	−0.720
0.389	0.606	0.693
0.818	−0.573	0.042
$\mathbf{A}^{63}$ tensor		
-16.1 ± 0.8	-57.5 ± 5.0	97.6 ± 2.5
0.459	0.494	−0.738
0.459	0.580	0.673
0.761	−0.648	0.040

describing the Zeeman and hyperfine (HF) interactions with the respective tensors **g** and $\mathbf{A}_i$, where the index i discerns the isotopes Cu^{63} and Cu^{65}, both with $I = 3/2$ nuclear spin (natural abundances 69.2 and 30.8%, nuclear g-factors 1.484 and 1.588), μ_B being the Bohr magneton. The resolved fourfold hyperfine structure due to Cu^{63} and some components due to Cu^{65} are shown in figure 3 for a general orientation of the magnetic field $\boldsymbol{B}$. The various Cu^{63} HF multiplets are due to families of magnetically non-equivalent, differently oriented centres containing the Cu^{63} isotope, while the assigned Cu^{65} lines are non-overlapping wing components of similar HF multiplets due to similar Cu^{65} centres. The relative intensities correspond to the natural abundances of both isotopes, and the ratio of the HF splittings to the ratio of their nuclear g-factors. The presence of altogether eight such centre families, discernable for general orientations of the magnetic field, proves that the local centre symmetry is C_1. In this case, for orientations of the magnetic field exactly within a crystallographic plane, the expected number of discernable centre families reduces to four, for $\boldsymbol{B} \parallel [100]$ and $\boldsymbol{B} \parallel [110]$ there remain only two, and for $\boldsymbol{B} \parallel \boldsymbol{c}$ all centres are magnetically equivalent. For most orientations of the magnetic field, strong overlap prevents the unique assignment of the components. The angular dependence of the Cu^{63} EPR spectra in the crystallographic planes is presented in figure 4. In the zx plane (figure 4(a)) the experimental points correspond to four HF quartets, though most lines show additional splittings due to a small misalignment of the sample. The corresponding components of the two quartets in the high-field lobes are separated by less than 4 mT, and those in the low-field part even less. In the xy plane (figure 4(b)) the extremal positions of all observed lines occur for directions very near to $\boldsymbol{B} \parallel [110]$ and the splittings between pairs of hyperfine quartets are smaller than 1 mT. In fact, the splittings due to centre inequivalence inside the xy plane and those attributable to sample misalignment are of the same magnitude in our experiments. However, in-plane splitting has to disappear for $\boldsymbol{B} \parallel [110]$, while the misalignment in our case clearly has different symmetry properties, so a careful study of the wing components allowed us to make convincing assignments of four (pair-wise nearly coinciding) in-plane HF quartets, despite their additional splittings due to sample misalignment. The lines in figure 4 were simulated using the fitted values of the spin-Hamiltonian tensor parameters given in table 1 (the program used was V G Grachev's 'Visual EPR'). The errors of the parameter values could be estimated by assuming maximal splittings reconcilable with the experimental data.

As expected for a centre that is well localized on one ion, the principal directions of the **g** and $\mathbf{A}^{63}$ tensors nearly coincide, the deviation being within 6°. The directions corresponding to the smallest g-value and the largest HF splitting (third principal axes) show an even smaller deviation (<2°), and are within a few degrees perpendicular to a {110}-type plane approximately containing all other eigenvectors (see figure 1(a)). This property corresponds to the small splittings observed in the angular dependence of the EPR spectra inside the crystallographic planes, and indicates that the Cu^{2+} centre

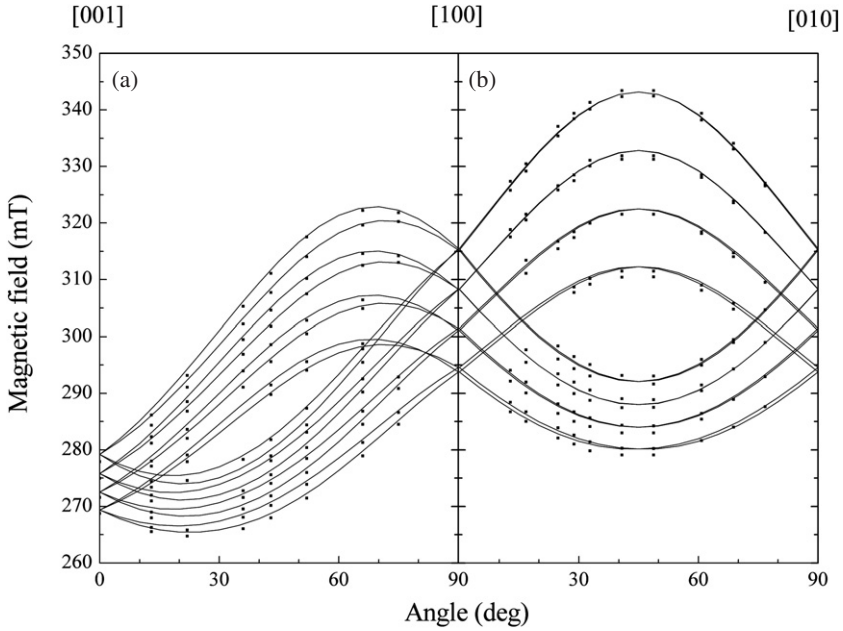

Figure 4. Angular dependence of the EPR line positions in the zx (a) and xy (b) planes. The points correspond to the experimental line positions where small splittings, if clearly attributable to sample misorientation, are averaged out. The lines were calculated using the data in table 1.

Table 2. Distances and position vectors of the four nearest oxygen neighbours of a Li^+ site with respect to this site [1]. The chosen Li^+ site corresponds to the one shown in figure 1(a) and (b) with cell coordinates $x/a = y/a = 0.342$ and $z/c = 0.36$, where $a = 9.47$ Å and $c = 10.26$ Å are the lattice constants. Also included are a possible relaxation vector **S** of the Cu^{2+} substituted at this Li^+ site and the changed position vectors of its oxygen neighbours.

Position vectors	O^1	O^2	O^3	O^4	$\mathbf{S} = \frac{1}{2}(O^1 + O^2)$	$O^2 - \mathbf{S} = -(O^1 - \mathbf{S})$	$O^3 - \mathbf{S}$	$O^4 - \mathbf{S}$
r (Å)	1.815	2.08	2.15	2.28	0.75	1.81	2.83	2.18
x/r	0.475	−0.842	0.432	−0.859	−0.594	−0.722	0.485	−0.696
y/r	−0.851	0.446	0.004	−0.245	−0.411	0.683	0.112	−0.115
z/r	0.226	0.301	−0.902	−0.450	0.692	0.113	−0.867	−0.709

that is observed has an approximate symmetry involving a {110}-type plane. This is an accidental property, somewhat unexpected in the $Li_2B_4O_7$ lattice, where there are no sites whatsoever with {110} mirror symmetry: in fact, all mirror planes of the point group C_{4v} of the lattice only correspond to glide planes of its space group, and there are no [110]-type symmetry axes either.

The most straightforward substitution site for Cu is the Li site. According to the x-ray diffraction analysis [1], the single type of Li site in the $Li_2B_4O_7$ lattice, though accidentally situated in a {110}-type glide plane, still has only C_1 local symmetry with a strongly distorted tetrahedral coordination (see figures 1(a) and (b)). As confirmed by EPR investigations of Cu^{2+} centres in other oxides (see e.g. [10–13]), the main principal axes of the spin-Hamiltonian tensors tend to point towards the nearest oxygen neighbour or neighbours. The positions of the four nearest oxygen neighbours of a Li site in $Li_2B_4O_7$, calculated from the diffraction data [1], are given in table 2 and are shown in figures 1(a) and (b). The first and second oxygen neighbours form an O^1–Li–O^2 angle of 135°, where the O^1–O^2 direction is within 6.9° parallel to a [110] direction. Upon substitution of Cu^{2+} for Li^+, some relaxation may be expected due to the larger charge and more covalent character of Cu^{2+}. Assuming a relaxation of the Cu^{2+} ion roughly towards the midpoint of the line connecting O^1 and O^2, the distances to these ligands may be slightly reduced. The positions of the ligands with respect to such a relaxed midpoint position are also included in table 2. Comparing the various ligand position vectors with the eigenvectors of the spin-Hamiltonian tensors given in table 1, excellent agreement can be found for the hypothetically relaxed case. In fact, the vectors pointing to the first two ligands are parallel within 3.7° to the main principal axis of the **g** tensor corresponding to the smallest g-value, $g_3 = 2.0265$. The third nearest ligand in the relaxed case, O^4, is situated in a direction that makes an angle of 23° with the principal axis corresponding to $g_1 = 2.515$. Taking into account that the ligand position vectors, unlike the eigenvectors, are strongly non-orthogonal, this comparison may also be considered to be quite satisfactory. Though this agreement cannot be considered as a proof for the relaxation to be exactly of this type, it still demonstrates that substitution at a relaxed Li site may reasonably explain the experimental results. These and all other observed properties of the Cu^{2+} defect should be checked by detailed calculations of the electronic structure.

Table 3. Properties of $3d^9$ centres in some oxides. Principal values of HF tensors are given in units of 10^{-4} cm^{-1}, JT stands for Jahn–Teller distortion, and subscripts in the centre model indicate substitution sites. Where available, suggestions for the type of ground state are also given with the model (an error in the final part of [12] has been corrected).

Matrix: ion	g_1	g_2	g_3	A_1	A_2	A_3	Site symmetry	Additional distortion	Model	Reference
$LiNbO_3$:Cu^{2+}	2.095	2.111	2.428	50.5	30.2	78	C_3 dist. octah.	Streched JT	Cu^{2+}_{Li} x^2-y^2	[11, 12]
$LiNbO_3$:Ni^{+}	2.246	2.217	2.061				C_3 dist. octah.	Compressed JT	Ni^{+}_{Li} $3z^2-r^2$	[12]
$PbWO_4$:Cu^{2+}(II)	2.497	2.282	2.002	12	20	93	C_4 dist. cubic.	JT?	Cu^{2+}_{Pb} xy?	[13]
$CdWO_4$:Cu^{2+}	2.496	2.302	2.012	0	15	82	C_2 3 × 2 oxyg.	JT?	Cu^{2+}_{Cd}	[10]
$MgWO_4$:Cu^{2+}	2.385	2.334	2.013	18	0	76	C_2 3 × 2 oxyg.	JT?	Cu^{2+}_{Mg}	[10]
$Li_2B_4O_7$:Cu^{2+}	2.515	2.220	2.027	−16.1	−57.5	97.6	C_1		Cu^{2+}_{Li}	This work

The two kinds of boron sites have strongly covalent bindings that are inappropriate for the substitution of Cu^{2+} ions, with three or four much closer oxygen neighbours than quoted for the Li site, which would force other orientations for the spin-Hamiltonian tensors than those observed. No other sites in the $Li_2B_4O_7$ lattice, even qualitatively reproducing the EPR results, could be found either.

The $3d^9$ electronic structure of the Cu^{2+} ion explains the single-hole character of the g values. The fivefold degeneracy of the ^{2}D ground state is completely lifted by the crystal field of C_1 symmetry. The average g values and HF splittings are similar to those measured for Cu^{2+} ions in other matrices. For comparison, some examples for $3d^9$ centres in various oxides are compiled in table 3 where, along with principal values of spin-Hamiltonian tensors, data on local structure and distortion are also given. As suggested also by the earlier data on $LiNbO_3$, the hole-type ground-state function tends to point towards the nearest oxygen neighbours [12]. As can be seen for $Li_2B_4O_7$, both spin-Hamiltonian tensors show larger anisotropies than found for the other matrices, which can be attributed to the much stronger distortion of the ligand spheres, related to the absence of symmetry elements (C_1) in our case. The ground state of Cu^{2+} in $Li_2B_4O_7$ may be assumed to contain an important contribution of a $3Z^2$-R^2-type state pointing towards the nearest (pair of) oxygen neighbours, with mostly XZ- and/or YZ-type d-admixtures, making the HF tensor non-axial. Any s-type admixture has to be small, as indicated by the isotropic part of the HF tensor, which is by far the smallest for $Li_2B_4O_7$ among the oxide matrices listed in table 3. Admixtures of the p-type, both in the ground and the low-lying s-type excited states of Cu^{2+}, may be significant, as suggested by the large g-shifts.

The obtained spin-Hamiltonian parameters presently do not allow us to make any conclusions about the presence of a charge-compensating defect. A natural compensator like a Li vacancy situated at 3.1 Å on a nearest-neighbour Li site would not qualitatively change the spectra. No other paramagnetic species in addition to the one described can be distinguished in the EPR spectra. The peak-to-peak EPR linewidth, attributed to unresolved HF interaction with the nuclei of matrix cations, is ∼0.5 mT, which seems to be smaller than the lineshift that the appearance of a nearest-neighbour Li vacancy might cause. For comparison see, for example, Mn^{2+} centres in a number of alkali chlorides only differing by an additional vacancy [14, 15]. Moreover, no angular dependence of the linewidth could be observed. This

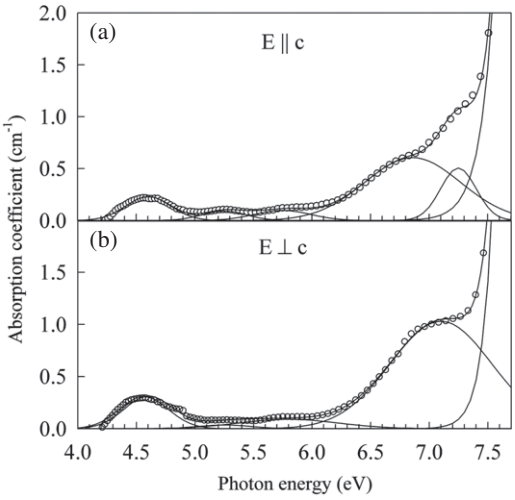

Figure 5. Absorption spectra of a $Li_2B_4O_7$:Cu crystal for (a) $\boldsymbol{E} \parallel \boldsymbol{c}$ and (b) $\boldsymbol{E} \perp \boldsymbol{c}$ at $T = 10$ K: circles—experimental curve; solid lines—decomposition of the experimental curve into Gaussian components and an exponential cutoff representing the matrix absorption edge.

indicates that the overwhelming majority of Cu^{2+} centres are essentially alike, either locally charge-compensated or not. It will be shown below that the other charge state of the dopant, Cu^{+}, is observed in luminescence studies showing intense parity-forbidden transitions, also indicating a low-symmetry substitution site.

3.2. *Optical properties*

The absorption, emission and excitation spectra of undoped and Cu-doped $Li_2B_4O_7$ single crystals for various orientations of the crystal $\boldsymbol{c}$ axis with respect to the electric vector of exciting light ($\boldsymbol{E} \parallel \boldsymbol{c}$ and $\boldsymbol{E} \perp \boldsymbol{c}$) are presented in figures 5 and 6. The absorption spectra were decomposed into Gaussian components and an exponential cutoff for the fundamental absorption edge at about 7 eV (figure 5). The absorption spectrum measured for $\boldsymbol{E} \parallel \boldsymbol{c}$ clearly shows five features centred at 7.25, 6.86, 5.75, 5.25 and 4.6 eV (figure 5(a)). For $\boldsymbol{E} \perp \boldsymbol{c}$, the two highest-energy peaks are not resolved, and a shoulder is observed at 7.1 eV instead (figure 5(b)). Both absorption spectra were measured up to the value of 8 cm^{-1} of the absorption coefficient. However, in order to better

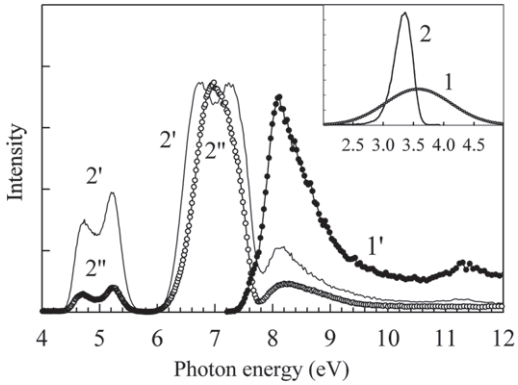

Figure 6. Time-integrated excitation spectra for the 3.65 eV (1′) and 3.35 eV (2′, 2″) emissions of $Li_2B_4O_7$ (1′) and $Li_2B_4O_7$:Cu (2′, 2″) crystals for $\boldsymbol{E} \parallel \boldsymbol{c}$ (1′, 2′) and $\boldsymbol{E} \perp \boldsymbol{c}$ (2″). In the inset: emission spectra of $Li_2B_4O_7$ (1) and $Li_2B_4O_7$:Cu (2) crystals at excitation energies of 8.0 eV (1) and 5.28 eV (2) for $\boldsymbol{E} \parallel \boldsymbol{c}$. $T = 10$ K.

demonstrate the impurity-related part, spectra are shown only up to 2 cm^{-1} in figure 5.

The emission spectra of $Li_2B_4O_7$:Cu reveal a strong band peaked at 3.35 eV (figure 6, curve 2) which substantially differs from the emission of STEs in the undoped $Li_2B_4O_7$ crystal (curve 1). The excitation spectrum of the 3.35 eV emission contains two groups of bands centred at 5 and 7 eV. The latter group is situated near the fundamental absorption edge and is obviously distorted on its short-wavelength side due to the host absorption. The shape of the spectrum and the intensity ratio of the two band groups are consistent with the absorption spectra and depend substantially on the orientation of the crystal with respect to the polarization vector of the exciting light (curves 2′, 2″). While two peaks at 4.75 and 5.2 eV are observed for the lower-energy group at both orientations, the higher-energy group is represented by two peaks at 6.77 and 7.23 eV for $\boldsymbol{E} \parallel \boldsymbol{c}$ and by only one broad band peaking at 7 eV for $\boldsymbol{E} \perp \boldsymbol{c}$. The excitation spectrum of the STE emission in undoped $Li_2B_4O_7$ is shown for comparison by curve 1′. The same characteristic shape is observed for $Li_2B_4O_7$:Cu in the high-energy part of the excitation spectrum of the 3.35 eV emission. The efficiency of the excitation grows in the region 7.8–8.3 eV strongly reduces towards 10 eV and then does not change significantly up to 20 eV. Excitation of $Li_2B_4O_7$:Cu by photons with energies higher than 8 eV produces a broad emission band that is identical to that of an undoped crystal (see curve 1). Its shape can be described by a single Gaussian function within experimental error, and in the first approximation the band can be considered to be elementary. No admixture of the 3.35 eV emission can be detected. This means that practically no energy transport by free charge carriers to the impurity centres responsible for the 3.35 eV emission takes place under excitation within the fundamental absorption region of $Li_2B_4O_7$, at least in the range 8–20 eV. The 3.35 eV band positions and half-widths completely coincide for excitation by 5.28 and 6.7 eV photons, and therefore both excitation band groups undoubtedly belong to the same luminescence centre. The Cu^+ ion is the most probable candidate for the emitting centre in $Li_2B_4O_7$:Cu. Accordingly, its $3d^9 4s \rightarrow 3d^{10}$ transitions have been considered to be responsible for the 3.35 eV emission band [7, 8]. The peaks in the absorption spectrum of the $Li_2B_4O_7$:Cu crystal mostly correspond to the bands observed in the excitation spectrum and are also related to the Cu^+ charge state of the dopant. However, there are some discrepancies with the low-energy part of the absorption spectrum containing the bands peaking near 4.5 and 5.7 eV. The 5.7 eV absorption band, having no counterpart in the excitation spectrum, obviously belongs to some uncontrolled impurity, while the distortion of the lowest-energy peak of Cu^+ (situated at 4.75 eV in the excitation spectrum) may be caused by the nonlinear response of the AXUV-100 photodiode at low energies.

To assign the excitation bands of the 3.35 eV emission, one has to refer to the energy-level scheme of the free Cu^+ ion. The ground state of the free Cu^+ ion is of the $3d^{10}$ configuration, while the lowest excited states are populated due to the $3d^{10} \rightarrow 3d^9 4s$ and $3d^{10} \rightarrow 3d^9 4p$ transitions, covering the energy ranges 2.7–3.3 eV and 8.3–9.2 eV, respectively [16]. The 4s electron is strongly antibonding toward the ligands and the 4p electron is partly bonding, therefore, upon incorporation into the crystal, the $3d^9 4s$ levels are raised in energy and the $3d^9 4p$ levels are lowered [17]. Taking this into account and also comparing our results in $Li_2B_4O_7$:Cu with those published for Cu-doped alkali halide crystals (AHCs) [17, 18], one can ascribe the group of absorption and excitation bands near 5 eV to the $3d^{10} \rightarrow 3d^9 4s$ transitions and that near 7 eV to the $3d^{10} \rightarrow 3d^9 4p$ transitions of the Cu^+ centre. This is the first observation of an allowed d $\rightarrow$ p transition in Cu^+-doped borate systems. The structure of the corresponding excited term and its anisotropy is the subject of future investigations. The $3d^{10} \rightarrow 3d^9 4s$ transition is parity- and spin-forbidden, but may be partly allowed due to off-centre displacements of the Cu^+ ion, as found for several AHCs [17, 18], or due to the original low symmetry of the $Li_2B_4O_7$ crystal field at a site lacking inversion and even mirror symmetry. The generally forbidden $3d^{10} \rightarrow 3d^9 4s$ transitions (near 5 eV) have a surprisingly high relative intensity with respect to the allowed $3d^{10} \rightarrow 3d^9 4p$ transitions (at 7 eV) and are strongly anisotropic in $Li_2B_4O_7$:Cu. The position (peaks at 4.75 and 5.2 eV) and the splitting (∼0.45 eV) of the $3d^9 4s$ term are close to those reported for those AHCs, in which the Cu^+ ion occupies off-centre positions at a cation site [18]. Accordingly, a substitution site of rather low symmetry is expected in the case of $Li_2B_4O_7$:Cu. This assumption is in good accordance with the above-described results of the EPR study of Cu^{2+} ions in the same crystal. Thus, the properties of the absorption and excitation spectra of Cu^+ seem to support the straightforward assumption that, because of its similar charge and ionic character, Cu^+ substitutes for Li^+ at or near to the cation site of C_1 symmetry and does not enter the covalent B–O network. However, the exact position of Cu^+ in its ground state cannot be verified with the methods used in the present work.

The alternatives for the Cu^+ ion with a simple low-symmetry site on the one hand and off-centre positions on the other hand can be discerned by the study of the emission decay kinetics. The temperature dependence of the decay kinetics of

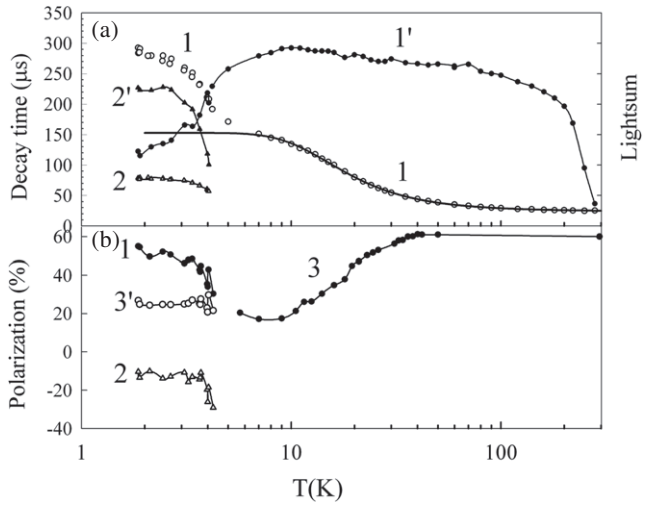

Figure 7. (a) Temperature dependences of the decay times (1, 2) and light sums (1′, 2′) of two decay components of the 3.35 eV emission under excitation by 5.2 eV photons for a $Li_2B_4O_7$:Cu crystal. Line 1 has been calculated to fit data between 6 and 297 K using the triplet state parameters given in the text. All other lines are only guides for the eye. (b) Temperature dependences of the polarization degree (P) of the same steady-state emission (3), of the slow (1) and anomalous fast (2) decay components of the low-temperature emission, and of their sum (3′). The excitation was non-polarized; the directions of both excitation and observation were normal to the c axis of the crystal.

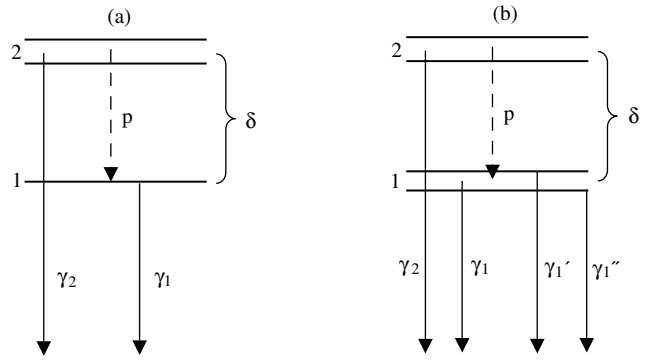

Figure 8. Scheme of the triplet relaxed excited state of the Cu^+ centre for the case of a low-symmetry crystal field (a) and for the case of tunnelling motion of the excited Cu^+ ion between off-centre positions for $T < 6$ K (b). Here, δ is the average energy distance between the crystal-field-split emitting level 2 and the tunnel-split metastable level 1. γ_1, γ_1', γ_1'' and γ_2 are radiative decay probabilities, and p is the probability of non-radiative transition.

the 3.35 eV emission of a $Li_2B_4O_7$:Cu crystal excited by 5.2 eV photons in the region 1.85–297 K is shown in figure 7(a). At room temperature, the decay kinetics are represented by a single component, whose decay time ($\tau = 25$ μs) is substantially shorter than that reported, for example, for NaF (90 μs), where Cu^+ is essentially an on-centre ion [17]. In the region 6–297 K, the temperature dependence of this single component shows a high-temperature plateau at 40–297 K, a sharp exponential increase of τ for lowering the temperature from 40 to 12 K, and a tendency to form a low-temperature plateau in the region 12–6 K (see the experimental points along curve 1 in figure 7(a)). Such a temperature dependence is typical of the so-called slow component observed for triplet relaxed states (see, e.g., [19, 20]). The triplet model is in good agreement with the experimental data on Cu^+ emission in cubic alkali halides, which has been attributed to the radiative decay of the relaxed ^3E_g state [17]. According to this model, the high-temperature plateau is caused by the complete thermal equilibrium between the components of the triplet, the upper doublet (called the emitting level) and the lower singlet (called the metastable level), at temperatures where the doublet is mainly responsible for the emission due to its substantially higher radiative decay probability. In the region of the low-temperature plateau, the emission is mainly due to the metastable singlet, while the emitting doublet is practically unpopulated [19]. Accepting the triplet model for the 3.35 eV emission of Cu^+ in $Li_2B_4O_7$, one should expect a splitting of the emitting doublet of the triplet state in two levels due to the low-symmetry crystal field at the Cu^+ substitution site. However, the energy of the splitting cannot be estimated from our measurements. In the Cu^+ emission in $Li_2B_4O_7$, there is no so-called fast non-equilibrium decay component originating from the emitting level, which is frequently seen for other systems with triplet relaxed excited states in the low-temperature interval starting from the region where the decay time of the slow component changes exponentially with decreasing temperature, and below that [19, 21]. For the case of Cu^+, this interval corresponds to the region between 6 and 40 K, where only a single slow component is observed. The absence of the non-equilibrium component means that there is no direct initial population of the emitting doublet during the relaxation from the non-relaxed $3d^9 4s$ term. A complete absence of the non-equilibrium decay component has been observed, for instance, also for In^+ centres in alkali halides [22] and for the triplet emission of self-trapped excitons in tungstate crystals [23].

Based on the procedure published in [19], from the temperature dependence of τ of the slow component in the region 6–297 K, the energy of the spin–orbit splitting of the triplet was calculated to be $\delta = 3.3 \times 10^{-3}$ eV, while for the radiative decay probabilities of the emitting doublet and the metastable singlet levels the values $\gamma_2 = 6 \times 10^4$ s^{-1} and $\gamma_1 = 6.5 \times 10^3$ s^{-1} have been obtained, respectively. For the probability of the non-radiative transition from the emitting to the metastable levels, we obtain $p = 3 \times 10^4$ s^{-1} (for a simplified scheme of the relaxed triplet state, see figure 8(a)). Curve 1 in figure 7(a) shows the calculated temperature dependence of the slow component using the above fitting parameters. While the agreement is perfect above 6 K, there is total disagreement for lower temperatures. Below 6 K the decay kinetics of the 3.35 eV emission splits into two components with a peculiar dependence of the decay times and light sums (curves 1, 1′, 2, 2′), none of which can be explained in terms of the simple triplet state model.

In our opinion the existence of two components below 6 K indicates a splitting of the metastable level and a doubling of the corresponding potential minimum. The corresponding scheme of the triplet excited state is shown in figure 8(b). The

very fact of the splitting of the single metastable level may seem unusual. On the other hand, the temperature dependence of the decay kinetics of the Cu^+ emission in $Li_2B_4O_7$ strongly resembles that reported for mercury-like ions of small radius in alkali halide crystals offering substitution sites of higher symmetry. For these ions the tunnel splitting of the metastable level of the triplet excited state could be established and attributed to the low-temperature tunnelling movement of the excited impurity ion between equivalent off-centre positions in the plane normal to the Jahn–Teller distortion axis [22]. The small-radius Cu^+ ion in its ground state also tends to occupy off-centre positions at liquid helium temperatures in a number of crystals with higher symmetry [18]. It can be assumed that this may also happen in its excited state, as required in our case. The mechanism of the splitting of a metastable level by tunnelling transitions is described in detail in [22].

While tunnel splitting seems to be the only possible cause for the splitting of a metastable singlet level, it is difficult to imagine two or more (nearly) equivalent off-centre positions for an excited Cu^+ ion occupying a low-symmetry Li^+ lattice site, despite the fact that the $Li_2B_4O_7$ lattice is less compact than that of Li_2O, where Li has fourfold tetrahedral coordination with a Li–O distance of 1.963 Å [24] (compare with the average 2.08 Å in $Li_2B_4O_7$; see table 2). Still, an argument in favour of such positions may be the existence of an approximate local symmetry. Indications for such an 'accidental' approximate symmetry of the Li site and the possible formation of a closely linear O–Cu–O chain have been discussed in section 3.1. However, the question about a possible off-centre configuration of excited Cu^+ ions has to be investigated further, considering another possible Cu^+ site as well: an interstitial site situated along the C_2 axis at an appropriate position between two B_4O_7 groups (see figure 1(a)). An interstitial position, e.g. ∼1.7 Å below the oxygen ion on the C_2 axis, would have eight further oxygen neighbours, all roughly at 3.1 Å, two boron sites at ∼2.3 Å and two Li sites at ∼2.1 Å without considering displacements and possible additional defects like lithium vacancies. For such a site the local symmetry is C_2. Consequently, two equivalent off-axis positions manifested in the Cu^+ excited state at low temperatures may be assumed. While this alternative may require unusually large relaxations and displacements, it contains the off-centre scenario as an inherent property supported by the twofold symmetry and elongated shape of the B_4O_7 unit. The latter model would also mean that Cu^+ and Cu^{2+} occupy somewhat different positions. However, this would not contradict present knowledge on this system.

Irrespective of the choice between the two above-described alternatives for the Cu^+ site, the assumed tunnel splitting of the metastable level can be estimated from the low-temperature data obtained below 6 K. Applying a two-level model similar to the triplet state model [19] but choosing as active levels only the tunnel-split levels instead of the metastable and emitting levels, the tunnel splitting can be estimated as 5×10^{-4} eV, which is almost an order of magnitude smaller than the spin–orbit splitting $\delta = 3.3 \times 10^{-3}$ eV derived above. Note that, considering the tunnel splitting of the metastable level, δ has to be interpreted as an average distance of the split emitting doublet and the tunnel-split metastable level, while γ_1 is the radiative probability of the metastable state under the condition that the tunnel sublevels are averaged out by thermal transitions. The probability of the radiative decay of the lowest tunnel sublevel can be estimated as $\gamma_1'' = 3.5 \times 10^3\ s^{-1}$, which is smaller than γ_1, as expected. The decay probability γ_1' of the upper sublevel cannot be calculated with sufficient precision due to the temperature interval where both tunnel components are observed being too short.

Also, the polarization properties of the 3.35 eV emission show features paralleling the results on decay kinetics. At room temperature the degree of polarization (P) is 60%, irrespective of the polarization of the exciting light, and does not depend on the emission wavelength within the whole emission band. It remains unchanged in the region of 297–40 K, where thermal equilibrium between the emitting and metastable levels of the triplet is maintained. In the region from 40 to 12 K, where the population of the emitting level gradually decreases and the decay time of the emission increases approaching the low-temperature plateau, the degree of polarization decreases steeply to about 20%. This means that electronic transitions from the emitting and metastable levels of the triplet relaxed excited states of Cu^+ ions have on average different orientations with respect to the crystal axis $\boldsymbol{c}$. In the region 6–1.85 K, where the decay kinetics of the 3.35 eV emission splits into two components, the polarization degree of the slower component approaches 60%, while that of the faster one reaches −10%, thus indicating that the corresponding transition takes place in the plane normal to the $\boldsymbol{c}$ axis. This is indicative of different polarization properties of the two components of the tunnel-split metastable level. Note that the degree of polarization of the emission coming from the lowest tunnel sublevel is the same as that of the whole triplet system in thermal equilibrium. Such behaviour is characteristic of tunnel sublevels, where the lowest one tends to display the symmetry properties possessed by the centre-symmetric state (see [22]). The polarization degree of the sum of both components (figure 7(b), curve 3′) is the same as that of the 3.35 eV emission in the region 6–12 K, where the splitting is not yet observable. Further investigations, including a group theoretical analysis of the data and an optically detected magnetic resonance study, are necessary to fully understand the effects that are observed.

4. Conclusion

The analysis of the results described leads to the conclusion that each charge state of the Cu dopant forms a well-defined low-symmetry species in the $Li_2B_4O_7$ lattice, and does not enter the covalent B–O network. Cu^{2+} has been shown by EPR to substitute at the Li^+ site, with an appreciable relaxation of the site and its surroundings which is inevitable because of the surplus charge of the dopant ion and the low (C_1) symmetry of the substitution site being well established for the Cu^{2+} species.

The temperature dependence of the decay kinetics of the Cu^+-related emission indicates that the relaxed excited state

of the Cu^+ centres is of triplet nature. A splitting of the metastable level of the Cu^+ triplet excited state is found for temperatures below 6 K, leading to the assumption about off-centre displacements of the Cu^+ ion in its excited state. This can be caused either by an accidental approximate symmetry of the Li^+ site (the seemingly trivial assumption for the substitution site of a monovalent cation) or by an interstitial position of Cu^+ with an average C_2 symmetry between two B_4O_7 groups.

The presence of additional defects, in particular charge compensators like nearby Li vacancies, cannot be excluded. To answer these and other open questions, further detailed experimental and theoretical work is required.

Acknowledgments

This work was supported by the Estonian Science Foundation (grant 7274 and post-doc grant 0072J) and the European Community—Research Infrastructure Action under the FP6 'Structuring the European Research Area' Programme (through the Integrated Infrastructure Initiative 'Integrating Activity on Synchrotron and Free Electron Laser Science'). Grants from the Hungarian Scientific Research Fund (K60086 and T037669) and the Cooperation Program between the Estonian and Hungarian Academies of Sciences are also acknowledged.

References

[1] Krogh-Moe J 1962 *Acta Crystallogr.* **15** 190
[2] Antonyak O T, Burak Ya V, Lyseiko I T, Pidzyrailo N S and Khapko Z A 1986 *Opt. Spectrosc.* **61** 345
[3] Ogorodnikov I N, Pustovarov V A, Kruzhalov A V, Isaenko L I, Kirm M and Zimmerer G 2000 *Phys. Solid State* **42** 464
[4] Malovichko G I, Grachev V G and Matkovskii A O 1991 *Fiz. Tverd. Tela* **33** 1966
Malovichko G I, Grachev V G and Matkovskii A O 1991 *Sov. Phys.—Solid State* **33** 1107 (Engl. Transl.)
[5] Malovichko G I, Vitruk L E, Yurchenko N Yu, Burak Ya V, Grachev V G, Matkovskii A O and Sugak D 1992 *Fiz. Tverd. Tela* **34** 509
Malovichko G I, Vitruk L E, Yurchenko N Yu, Burak Ya V, Grachev V G, Matkovskii A O and Sugak D 1992 *Sov. Phys.—Solid State* **34** 272 (Engl. Transl.)
[6] Prokic M 2002 *Radiat. Prot. Dosim.* **100** 265
[7] Ishii M, Kuwano Y, Asai T, Senguttuvan N, Hayashi T, Kobayashi M, Oku T, Sakai K, Adachi T, Shimizu H M and Suzuki J 2003 *J. Cryst. Growth* **257** 169
[8] Ignatovich M, Holovey V, Watterich A, Vidóczy T, Baranyai P, Kelemen A and Chuiko O 2004 *Radiat. Meas.* **38** 567
[9] Nagirnyi V, Jönsson L, Kirm M, Kotlov A, Lushchik A, Martinson I, Watterich A and Zadneprovski B I 2004 *Radiat. Meas.* **38** 519
[10] Sroubek Z 1966 *J. Chem. Phys.* **44** 3078
[11] Kobayashi T, Muto K, Kai J and Kawamori A 1979 *J. Magn. Reson.* **34** 459
[12] Corradi G, Polgár K, Bugai A A, Zaritskii I M, Rakitina L G, Grachev V G and Derjugina N I 1986 *Fiz. Tverd. Tela* **28** 739
Corradi G, Polgár K, Bugai A A, Zaritskii I M, Rakitina L G, Grachev V G and Derjugina N I 1986 *Sov. Phys.—Solid State* **28** 412 (Engl. Transl.)
[13] Hofstaetter A, Laguta V V, Meyer B K, Nikl M, Rosa J and Zhu R Y 2004 *Radiat. Meas.* **38** 703
[14] Watkins G W 1959 *Phys. Rev.* **113** 79
[15] Watkins G W 1959 *Phys. Rev.* **113** 91
[16] Moore C E 1952 *Atomic Energy Levels, Natl. Bur. Std. (U.S.) Circ.* vol 2, p 46
[17] McClure D S and Weaver S C 1991 *J. Phys. Chem. Solids* **52** 81
[18] Payne S A 1987 *Phys. Rev.* B **36** 6125
[19] Hizhnyakov V, Liidja G, Nagirnyi V, Soovik T and Zazubovich S 1983 *Phys. Status Solidi* b **120** 105
[20] Hizhnyakov V and Kristoffel N 1984 Jahn–Teller mercuri-like impurities in ionic crystals *The Dynamical Jahn–Teller Effect in Localized Systems* ed Yu Perlin and M Wagner (Amsterdam: Elsevier Sci. Publishing) pp 383–438
[21] Nagirnyi V, Stolovich A, Zazubovich S and Jaanson N 1994 *Phys. Rev.* B **50** 3553
[22] Liidja G, Nagirnyi V, Soovik T and Zazubovich S 1989 *Phys. Status Solidi* c **152** 563
[23] Babin V, Bohacek P, Bender E, Krasnikov A, Mihokova E, Nikl M, Senguttuvan N, Stolovits A, Usuki Y and Zazubovich S 2004 *Radiat. Meas.* **38** 533
[24] Rodeja J G, Meyer M and Hayoun M 2001 *Modelling Simul. Mater. Sci. Eng.* **9** 81 http://www.cond-mat.physik.uni-mainz.de/∼horbach/cecam2005/cecam_hayoun.ppt#1